G13A Substitution Affects the Biochemical and Physical Properties of the Elongation Factor 1α. A Reduced Intrinsic GTPase Activity Is Partially Restored by Kirromycin†

Mariorosario Masullo,‡,§ Piergiuseppe Cantiello,§ Barbara de Paola,§ Francesca Catanzano,|| Paolo Arcari,*,§ and Vincenzo Bocchini§,⊥

Dipartimento di Scienze Farmacobiologiche, Università degli Studi di Catanzaro Magna Graecia, Complesso Ninì Barbieri, Roccelletta di Borgia, I-88021 Catanzaro, Italy, Dipartimento di Biochimica e Biotecnologie Mediche, Università di Napoli Federico II, and CEINGE, Biotecnologie Avanzate Scarl, via S. Pansini 5, I-80131 Napoli, Italy

Received July 20, 2001; Revised Manuscript Received October 19, 2001

ABSTRACT: The G13A substitution in the G13XXXXGK[T,S] consensus sequence of the elongation factor 1α from the archaeon *Sulfolobus solfataricus* (*Ss*EF-1α) was introduced in order to study the reasons for selective differences found in the homologous consensus element AXXXXGK[T,S] of the other elongation factor EF-2 or EF-G. In a previous work, it was shown that the main effect of the A26G mutation was the activation of the intrinsic GTPase of *Ss*EF-2 [De Vendittis, E., Adinolfi, B. S., Amatruda, M. R., Raimo, G., Masullo, M., and Bocchini, V. (1994) *Eur. J. Biochem. 262*, 600−605]. In this work, we found that, compared to the wild-type factor (*Ss*EF-1α wt), G13A*Ss*EF-1α shows (i) a reduced rate of [^{3}H]Phe polymerization that was probably due to its reduced ability to form a ternary complex with heterologous aa-tRNA and (ii) a reduced intrinsic GTPase activity that was stimulated by high concentrations of NaCl (GTPase^{Na}) [Masullo, M., De Vendittis, E., and Bocchini, V. (1994) *J. Biol. Chem. 269*, 20376−20379]. In addition, G13A*Ss*EF-1α showed an increased affinity for GDP and GTP. Surprisingly, the decreased intrinsic GTPase^{Na} of G13A*Ss*EF-1α can be partially restored by kirromycin, an effect not found for *Ss*EF-1α wt. The temperature inducing a 50% denaturation of G13A*Ss*EF-1α was somewhat lower (−5 °C) than that of *Ss*EF-1α wt, and the decrease in its thermophilicity was slightly more accentuated (−10 °C). These results indicate that the nature of the residue in position 13 is important for the functional and physical properties of *Ss*EF-1α.

The elongation factor 1α from the hyperthermophilic archaeon *Sulfolobus solfataricus*[1] is a GTP-binding protein; thus, it is endowed with a GTPase activity (*1*−*3*). Its amino terminal displays the selective homologies of the guanine nucleotide-binding proteins (*3*). These GTPases are characterized by the consensus sequences [G,A]XXXXGK[T,S], DXXG, and NKXD that are involved in the binding of GDP or GTP (*4*). Furthermore, the three-dimensional (3D) structures of eubacterial EF-Tu (*5*−*9*) and EF-G (*10, 11*) and that of eucarial EF-1α (*12*) show that the guanine nucleotide-binding domains share similar structural features (*13, 14*). Interestingly, however, in the sequence motif [G,A]XXXXGK, the first amino acid residue is alanine in EF-2 and EF-G, whereas in EF-1α and EF-Tu, this position is occupied by glycine (*4*). In the 3D structure of EF-Tu, in either the GDP- or the GTP-bound form, this glycine is not directly involved in the binding of phosphate (*14, 15*). Therefore, it appears interesting to investigate its role in the functional properties of the translational elongation factor EF-1α from the archaeon *S. solfataricus* (*Ss*EF-1α). In a previous work, it was found that A26G substitution activated the intrinsic GTPase of *Ss*EF-2 (*16*). Our results show that G13A replacement affects the affinity of *Ss*EF-1α for guanine nucleotides as well as the ability to hydrolyze GTP and sustain poly(Phe) synthesis. In addition, G13A mutation makes *Ss*EF-1α sensitive to the antibiotic kirromycin, a typical inhibitor of eubacterial but not of archaeal or eucarial protein synthesis.

MATERIALS AND METHODS

Chemicals, Enzymes, and Buffers. Restriction enzymes, modifying enzymes, labeled compounds, and chemicals were used as already reported (*17*); standard molecular biology techniques were performed as previously described (*18*).

The following buffers were used: buffer A was 20 mM Tris HCl (pH 7.8), 50 mM KCl, and 10 mM $MgCl_2$; buffer B was 20 mM Tris HCl (pH 7.8), 10 mM $MgCl_2$, and 1 mM DTT.

Plasmid Construction, Expression, and Purification of the Mutant G13ASsEF-1α. The E8 plasmid containing the gene

† This work was supported by CNR, MURST (Rome, Italy), and the European Community Biotechnology Program (Contract BIO4-CT97-2188).

* Corresponding author. Phone: +39 081 7463120. Fax: +39 081 7463653. E-mail: arcari@dbbm.unina.it.

‡ Università deli Studi di Catanzaro Magna Graecia.

§ Università di Napoli Federico II.

|| CEINGE, Biotecnolgie Avanzate Scarl.

⊥ Died on June 28, 2001.

[1] Abbreviations: EF, elongation factor; *Ss*, *Sulfolobus solfataricus*; *Ec*, *Escherichia coli; Tt*, *Thermus thermophilus*; *Ta*, *Thermus aquaticus*; G13A*Ss*EF-1α, *Ss*EF-1α carrying the G13A substitution; GTPase^{Na}, intrinsic GTPase of *Ss*EF-1α triggered by 3.6 M NaCl; CD, circular dichroism.

10.1021/bi015598h CCC: $22.00
Published on Web 12/14/2001

encoding the wild-type elongation factor from *S. solfataricus* 1α (*Ss*EF-1α wt) (*17*) was used as a template with two self-complementary primers A_{34}TA GCT CAC GTC GAT CAC GG, carrying the G38C base substitution, as numbered from the EF-1α starting codon. The new plasmid was synthesized by polymerase chain reaction and used to transform *Escherichia coli* BL21 (DE3) (*19*). An overnight cell culture grown at 37 °C in an L broth containing 100 μg/mL of ampicillin was diluted 1:100 and grown up to 0.7 absorbance units at 600 nm. Induction (3 h) was performed by adding isopropyl-β-D-thiogalactopyranoside up to a final concentration of 0.4 mM. The bacterial cells were collected by centrifugation, resuspended in buffer A (6 mL/g of wet cells) containing 15% glycerol and 1 mM phenylmethanesulfonyl fluoride, and disrupted by pressure using a constant cell disruption system (Constant Systems Ltd., U.K.) at 1.5 kbar. The G13A*Ss*EF-1α mutant was purified according to the procedure already reported for *Ss*EF-1α wt (*17*). Briefly, the postribosomal supernatant was treated for 30 min at 70 °C, and most of the *E. coli* denaturated proteins were removed by centrifugation. The supernatant was dialyzed against 25 mM MES/KOH (pH 6.2) and applied onto a MonoS column equilibrated with the same buffer. G13A*Ss*EF-1α was eluted by a 0−400 mM KCl gradient at about 200 mM KCl. Fractions containing a single protein band on sodium dodecyl sulfate−polyacrylamide gel electrophoresis (SDS−PAGE) were pooled, concentrated with Aquacide IIa, dialyzed against buffer A containing 50% (v/v) glycerol and 10 μM GDP, and stored at −20 °C.

SsEF-1α Assays. The poly(U)-directed poly(Phe) synthesis and isolation of total tRNA and ribosomes from *S. solfataricus* were performed as already described (*20*). The effect of 100 μM kirromycin on poly(Phe) synthesis was checked kinetically at 75 °C.

The preparation of Phe-tRNA^{Phe}, the formation of the ternary complex G13A*Ss*EF-1α·[γ-^{32}P]GTP·*Ec*Phe-tRNA^{Phe}, was carried out as already described (*21*). Protection against the spontaneous deacylation of [^{3}H]Phe-tRNA^{Phe} and [^{3}H]-Val-tRNA^{Val} was obtained as previously reported (*22*).

The ability of G13A*Ss*EF-1α to form a binary complex with [^{3}H]GDP was tested as described (*1*). The number of [^{3}H]GDP binding sites and the apparent equilibrium dissociation constant (K_d') of the binary complex between G13A*Ss*EF-1α·[^{3}H]GDP were determined by a Scatchard plot; K_d' for GTP was obtained by competitive-binding experiments in the presence of 25 μM [^{3}H]GDP (specific activity of 530 cpm/pmol) at different GTP concentrations; the apparent dissociation rate constant of the G13A*Ss*EF-1α·GDP complex was determined as already reported (*1*). The effect of *Ss*EF-1β on the [^{3}H]GDP/GDP and [^{3}H]GDP/GTP exchange on the preformed G13A*Ss*EF-1α·[^{3}H]GDP complexes was evaluated at 60 °C as previously described (*23*).

The GTPase^{Na} activity of G13A*Ss*EF-1α was measured in the presence of 3.6 M NaCl (*2*) and in the presence or absence of kirromycin. Unless otherwise indicated, the reaction mixture contained 1−3 μM G13A*Ss*EF-1α and 50 μM [γ-^{32}P]GTP (specific activity of 150−300 cpm/pmol) in buffer B. The reaction was followed kinetically up to 30 min at 60 °C; the amount of $^{32}P_i$ released, the catalytic constant of GTPase^{Na}, the affinity for [γ-^{32}P]GTP, and the inhibition constants by GDP and Gpp(NH)p of GTPase^{Na} were determined as already reported (*20*).

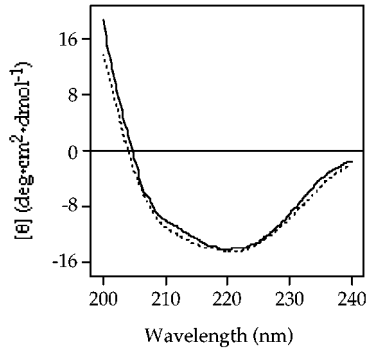

FIGURE 1: Far-UV CD spectra of *Ss*EF-1α and G13A*Ss*EF-1α. Measurements were recorded at 25 °C at a protein concentration of 0.1 mg/mL in a 10 mM Tris HCl buffer (pH 7.5): *Ss*EF-1α, continuous line; G13A*Ss*EF-1α, dashed line.

Thermophilicity and Heat Stability of G13ASsEF-1α. The thermophilicity of G13A*Ss*EF-1α was checked by measuring GTPase^{Na} in the temperature range of 40−91 °C. At each temperature, the reaction was followed kinetically; at time intervals depending on the temperature, 40 μL aliquots were withdrawn and analyzed for the $^{32}P_i$ released (*2*). The data were treated according to the Arrhenius equation, and the energetic parameters of activation were calculated as reported (*23*).

Heat inactivation of G13A*Ss*EF-1α was evaluated by incubating a 4 μM protein in buffer A for 10 min at selected temperatures in the interval of 70−102 °C. Aliquots of 25 μL were cooled on ice for 30 min and then analyzed for their [^{3}H]GDP binding ability, and their residual GTPase^{Na} activity measured in a final volume of 100 and 200 μL, respectively, as described previously. Ultraviolet (UV) melting curves were obtained in the temperature range of 60−100 °C as previously reported (*21*). CD measurements were performed with a JASCO J-710 spectropolarimeter, calibrated with an aqueous solution of (+) camphorsulfonic acid-d_{10} at 290 nm. Far-UV CD spectra were recordered using a 0.1 cm cuvette at a time constant of 4 s and a 2 nm bandwidth. Thermal unfolding curves were determined at 222 nm in 10 mM Tris HCl (pH 7.0) with a scan rate of 1 K/min.

Molecular Modeling. The 3D structure of EF-Tu·GDP from *Thermus aquaticus* (*Ta*EF-Tu, Protein Data Bank entry code 1TUI) was used as a template to predict the effect of the G13A point mutation in *Ss*EF-1α by using the Swiss PDB viewer software (*24*).

RESULTS

SsEF-1α and G13ASsEF-1α Showed Identical Molecular Properties. Under either native (gel filtration) or denaturing (SDS−PAGE) conditions, purified G13A*Ss*EF-1α showed the same M_r as *Ss*EF-1α. In addition, at 25 °C, both *Ss*EF-1α and G13A*Ss*EF-1α showed almost overlapping CD spectra (Figure 1) with a minimum at 222 nm. This result suggested that both samples contained the same extent of secondary structure.

G13ASsEF-1α Supports Poly(Phe) Synthesis. The rate of poly[^{3}H]Phe synthesis catalyzed by G13A*Ss*EF-1α was about 1 order of magnitude slower than that elicited by *Ss*EF-1α (Figure 2A). Such a difference became smaller at increasing concentrations of the elongation factor (Figure 2B). The maximum rate of amino acid incorporation was almost

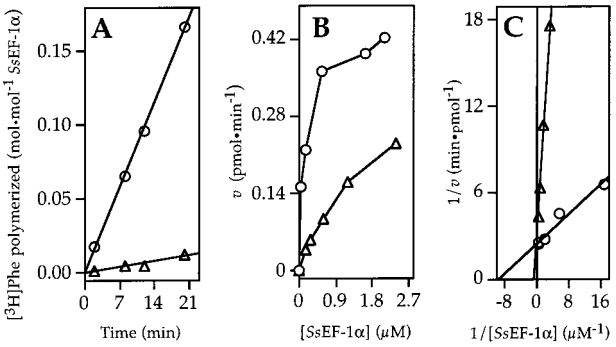

FIGURE 2: Poly(U)-directed poly(Phe) synthesis promoted by *Ss*EF-1α and G13A*Ss*EF-1α. (A) Time course of [^{3}H]Phe polymerization; 300 μL of the reaction mixture contained 25 mM Tris HCl (pH 7.5), 19 mM magnesium acetate, 10 mM NH_4Cl, 10 mM dithiotreitol, 1.6 mM GTP, 0.16 mg/mL poly(U), 3 mM spermine, 0.25 μM *Ss*ribosome, 80 μg/mL *Ss*tRNA, and 2.4 μM [^{3}H]Phe (specific activity of 24 120 cpm/pmol). The reaction was started by the addition of 0.5 μM final concentration of *Ss*EF-1α (○) or G13A*Ss*EF-1α (Δ) and carried out at 75 °C. At the times indicated, 70 μL aliquots were withdrawn, chilled on ice, and then analyzed for the amount of [^{3}H]Phe polymerized. (B) Effect of increasing concentration of *Ss*EF-1α and G13A*Ss*EF-1α. The reaction was allowed to proceed for 20 min under the experimental conditions as in panel A; v is the rate of poly[^{3}H[Phe polymerization. (C) Lineweaver−Burk plots of the data reported in panel B.

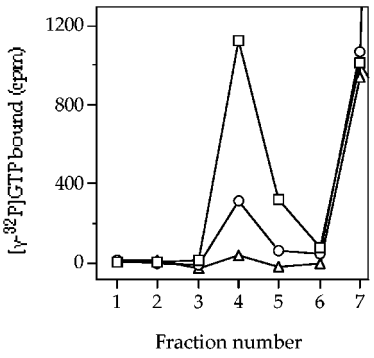

FIGURE 3: Interaction between *Ss*EF-1α, G13A*Ss*EF-1α, and *Ec*EF-Tu with *Ec*Phe-tRNA^{Phe}; 35 μL of buffer A contained 60 mM NH_4Cl, 0.2 μM SsEF-1α (○), G13ASsEF-1α (Δ), or EcEF-Tu (□) and 1 μM *Ec*Phe-tRNA^{Phe}, 1 μM [γ-^{32}P]GTP (specific activity of 6200 cpm/pmol), 1 mM phosphoenolpyruvate, and 40 μg/mL pyruvate kinase. The reaction mixture was incubated for 10 min at 0 °C, and then 30 μL was loaded onto a Sephadex G-25 column (0.4 × 15 cm) equilibrated with buffer A. The 100 μL fractions were collected and counted for radioactivity. Blanks run in the absence of *Ec*Phe-tRNA^{Phe} were subtracted.

identical for both the mutated and the wild-type enzyme (0.38 and 0.41 mol of [^{3}H]Phe polymerized (mol of enzyme)$^{-1}$ min^{-1}, respectively), but the concentration of G13A*Ss*EF-1α required to get half-maximum activity (K_{act}) was about 16-fold higher than that required by *Ss*EF-1α (1.732 and 0.105 μM, respectively; Figure 2C).

The ability of G13A*Ss*EF-1α to interact with aa-tRNA was tested by measuring the amount of ternary complex formed between heterologous *Ec*Phe-tRNA^{Phe}, [γ-^{32}P]GTP, and G13A*Ss*EF-1α under the experimental conditions already reported (*21*, *22*). As shown in Figure 3, *Ss*EF-1α wt, compared to *Ec*EF-Tu, showed a lower affinity toward *Ec*Phe-tRNA^{Phe} that was further reduced in the case of G13A*Ss*EF-1α. This behavior was confirmed by the lower ability of G13A*Ss*EF-1α versus *Ss*EF-1α wt to protect [^{3}H]-*Ec*Val-tRNA^{Val} and [^{3}H]*Ec*Phe-tRNA^{Phe} against spontaneous deacylation (not shown).

Table 1: Affinity of *Ss*EF-1α and G13A*Ss*EF-1α for Guanine Nucleotides at 60 °C[a]

	K_d'		k_{-1} GDP	k_{+1} GDP
	GDP (μM)	GTP (μM)	(min^{-1})	(μM^{-1} min^{-1})
*Ss*EF-1α	1.6	35	0.1	0.06
G13A*Ss*EF-1α	0.7	10	5.7	8.1

[a] k_{+1} was calculated as k_{-1}/K_d'.

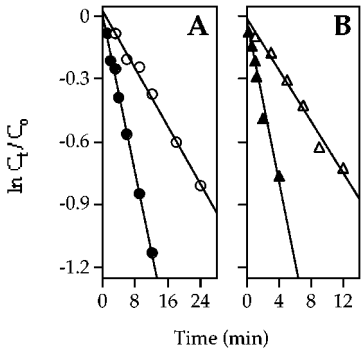

FIGURE 4: Effect of *Ss*EF-1β on the [^{3}H]GDP/GTP exchange on the preformed *Ss*EF-1α·[^{3}H]GDP and G13A*Ss*EF-1α·[^{3}H]GDP complexes. The preformed *Ss*EF-1α·[^{3}H]GDP and G13A*Ss*EF-1α·[^{3}H]GDP complexes were prepared by incubating 0.5 μM protein with 6 μM [^{3}H]GDP (specific activity of 2000 cpm/pmol) for 30 min at 60 °C. The exchange reaction (350 μL) was started by the addition of 2 mM GTP (empty symbols) or 2 mM GTP and 0.1 μM *Ss*EF-1β (filled symbols) and was followed kinetically by measuring the amount of residual radioactive complex in 45 μL aliquots. C_0 is the concentration of the radioactive binary complex at the time zero and C_t its concentration at the time t: panel A, *Ss*EF-1α; panel B, G13A*Ss*EF-1α.

Interaction of G13ASsEF-1α with GDP and GTP. As shown in Table 1, the affinity of G13A*Ss*EF-1α for GDP and GTP was about 2−3-fold higher as compared to *Ss*EF-1α. A more pronounced effect was observed for the dissociation and association rate constants of [^{3}H]GDP binding that for G13A*Ss*EF-1α were about 2 orders of magnitude higher as compared to *Ss*EF-1α.

The [^{3}H]GDP/GTP exchange rate on *Ss*EF-1α·[^{3}H]GDP became about 3 times faster in the presence of *Ss*EF-1β in the case of either *Ss*EF-1α·[^{3}H]GDP or G13A*Ss*EF-1α·[^{3}H]-GDP (Figure 4). A similar result was obtained for the [^{3}H]-GDP/GDP exchange reaction (not shown).

G13ASsEF-1α Supports a Reduced GTPase^{Na} Activity That Was Partially Restored by Kirromycin. *Ss*EF-1α is able to hydrolyze GTP in the presence of NaCl at molar concentrations (Figure 5A; *2*). The turnover rate of GTPase^{Na} elicited by G13A*Ss*EF-1α (Figure 5B) was significantly lower as compared to that of *Ss*EF-1α (Figure 5A). At 60 °C, the K_m for GTP and the k_{cat} of the reaction decreased by 17- and 8-fold, respectively; as a consequence, the catalytic efficiency of the GTPase^{Na} of G13A*Ss*EF-1α was 2 orders of magnitude lower as compared to that of *Ss*EF-1α (Table 2). As already found for *Ss*EF-1α, the GTPase^{Na} of G13A*Ss*EF-1α was competitively inhibited by GDP but with a lower efficiency as compared to *Ss*EF-1α.

Kirromycin did not stimulate the GTPase^{Na} of *Ss*EF-1α (Figure 5A). Vice versa, the antibiotic enhanced the rate of GTP hydrolysis by G13A*Ss*EF-1α, and the maximum stimu-

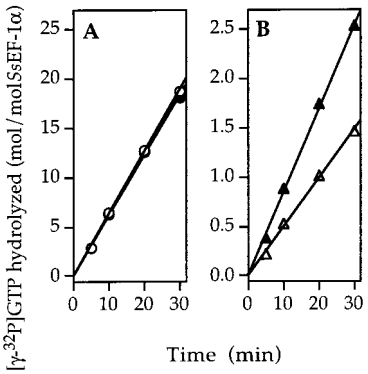

FIGURE 5: Effect of kirromycin on the GTPase^{Na} of *Ss*EF-1α and G13A*Ss*EF-1α; 230 μL of the reaction mixture contained 0.3 μM SsEF-1α (panel A) or 3 μM G13A*Ss*EF-1α (panel B) in the absence (empty symbols) or in the presence (filled symbols) of 50 μM kirromycin in buffer A containing 3.6 M NaCl and 50 μM [γ-^{32}P]-GTP (specific activity of 300 cpm/pmol). The reaction was carried out at 60 °C, and at the times indicated, 50 μL aliquots were withdrawn and analyzed for $^{32}P_i$ release as reported in the Materials and Methods section.

Table 2: Intrinsic GTPase of *Ss*EF-1α and G13A*Ss*EF-1α at 60 °C

	K_m (μM)	k_{cat} (min^{-1})	k_{cat}/K_m (min^{-1} μM^{-1})	$K_{i(GDP)}$ (μM)
*Ss*EF-1α	2.7	0.8	0.3	0.8
G13A*Ss*EF-1α	46.0	0.1	0.003	4.2

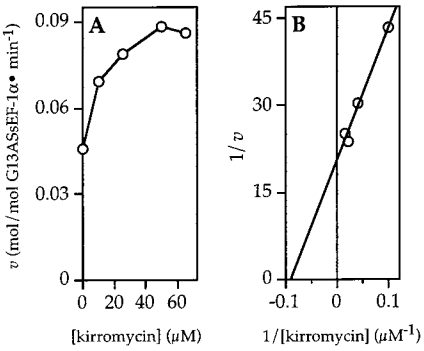

FIGURE 6: Affinity of G13A*Ss*EF-1α for kirromycin in the GTPase^{Na}. (A) The reaction mixture contained 3 μM G13A*Ss*EF-1α and was prepared as described in the legend to Figure 5 in the presence of kirromycin at the indicated concentration. The reaction was followed kinetically at 60 °C, and the slope of the linear part of each kinetics was plotted as a function of the kirromycin concentration. (B) The data reported in panel A were treated by the Lineweaver−Burk equation after the subtraction of the GTPase^{Na} activity of G13A*Ss*EF-1α in the absence of kirromycin.

latory effect was observed at around 40 μM kirromycin (Figure 6A); the concentration of kirromycin required for half-maximum activation was 10 μM (Figure 6B).

Thermophilicity and Thermostability of SsEF-1α Are Also to Some Extent Affected by G13A Substitution. The heat inactivation profile of the [^{3}H]GDP binding ability showed that G13A*Ss*EF-1α was half inactivated after exposure for 10 min at 91 °C (Figure 7A). This value was 3 °C lower than that required for the half inactivation of *Ss*EF-1α.

The stability of *Ss*EF-1α and its G13A mutant was evaluated by ultraviolet-monitored thermal denaturation (Figure 7B). The temperature for the half denaturation of G13A*Ss*EF-1α (87 °C) was close to that determined from the inactivation profile (Figure 7A) and was 5 °C lower than that observed during the denaturation of the wild-type

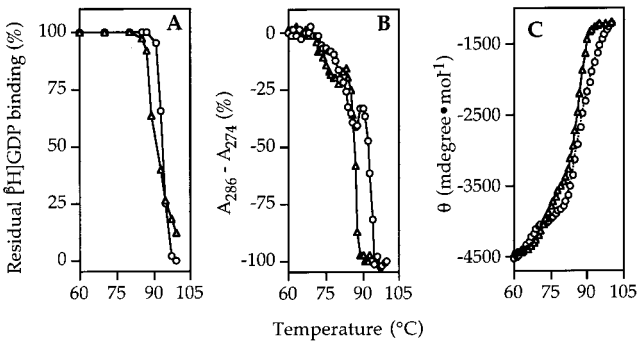

FIGURE 7: Heat stability of G13A*Ss*EF-1α and *Ss*EF-1α. Residual [^{3}H]GDP binding ability (panel A), UV melting curves (panel B), and CD denaturation curves (panel C) of *Ss*EF-1α (○) and G13A*Ss*EF-1α (Δ). For other details, see the Materials and Methods section.

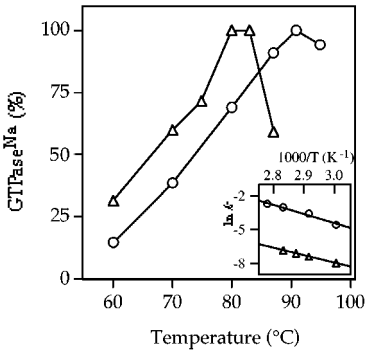

FIGURE 8: Thermophilicity of G13A*Ss*EF-1α and *Ss*EF-1α. The GTPase^{Na} activity was assayed as described in the legend to Figure 5 at the indicated temperatures and was reported as a percentage of the maximum GTPase^{Na}, calculated considering 4.0 and 0.064 mol of [γ-^{32}P]GTP hydrolyzed per minute per mole of protein for *Ss*EF-1α (○) or G13A*Ss*EF-1α (Δ), respectively. (Inset) Arrhenius analysis of the data in the range 60−80 °C for G13A*Ss*EF-1α and 60−87 °C for *Ss*EF-1α.

protein. The thermal stability of *Ss*EF-1α and G13A*Ss*EF-1α was also studied by measuring the loss of secondary structure by CD measurements at 222 nm. The temperatures for half denaturation observed in the cases for *Ss*EF-1α and G13A*Ss*EF-1α were 86 and 85 °C, respectively (Figure 7C).

The thermophilicity of the G13A mutant was compared to that of *Ss*EF-1α on the basis of GTPase^{Na} activity at increasing temperatures. G13A*Ss*EF-1α showed the highest activity at 80 °C, a temperature about 10 °C lower than that measured for *Ss*EF-1α, after inactivation occurred (Figure 8).

The analysis according to the Arrhenius equation in the rising part of the curves indicated that the values of the activation energy of GTPase^{Na} were 55.4 and 67.3 kJ mol^{-1} for the G13A mutant and *Ss*EF-1α, respectively (Figure 8, inset). The entropies of activation at 60 °C for the GTPase reaction-catalyzed *Ss*EF-1α and G13A*Ss*EF-1α were −90 and −154 J mol^{-1} K^{-1}, whereas the free energies of activation were 94 and 104 J mol^{-1}, respectively.

DISCUSSION

The GTP-binding proteins are characterized by the [G,A]-XXXXGK[T,S] consensus sequence. The first amino acid residue of this sequence is glycine in EF-Tu and EF-1α and in Ha-Ras p21, whereas it is alanine in elongation factors EF-G and EF-2 (*4*). To investigate the biochemical effects

depending on such a difference, a mutated *Ss*EF-1α carrying the G13A substitution was constructed, and its properties were compared to the effects caused in *Ss*EF-2 wt by the opposite A26G replacement in the corresponding consensus sequence (*16*).

The G13A mutation significantly reduced the efficiency of *Ss*EF-1α to sustain poly(Phe) synthesis (Figure 2). This behavior cannot be attributed to impairment by the G13A substitution of the nucleotide-exchange reaction because *Ss*EF-1*β* was able to accelerate the GDP/GTP exchange on G13A*Ss*EF-1α almost with the same efficiency as that for *Ss*EF-1α wt. The lower ability of G13A*Ss*EF-1α to stimulate poly(Phe) synthesis might depend on a much less efficient interaction of G13A*Ss*EF-1α with aa-tRNA, as studied using the heterologous aa-*Ec*tRNA (Figure 3). Alternatively, the reduced efficiency of G13A*Ss*EF-1α in poly(Phe) synthesis is the lower capability of G13A*Ss*EF-1α to hydrolyze GTP, as evaluated through GTPase^{Na} induced by a high-salt concentration (Table 2). The G13ASsEF-1α mutant binds GDP and GTP with affinities higher than those displayed by *Ss*EF-1α (Table 1). Such an increased affinity was more pronounced for GTP than for GDP. In the case of GDP, the increment might be ascribed to a higher value of k_{+1} with respect to k_{-1}. This finding suggested that the G13A mutation rendered more accessible the nucleotide-binding site on *Ss*EF-1α. An opposite effect was observed in the reciprocal mutation of *Ss*EF-2, where the A26G mutation causes a significant increase of K_d' for GDP (*16*). Contrary to the increased affinity for GTP and GDP, G13A*Ss*EF-1α displays, as compared to *Ss*EF-1α, a significantly reduced GTPase^{Na} characterized by a lower affinity for both GTP and GDP (compare K_m for GTP to K_i for GDP in Table 2) and by a reduction of its catalytic efficiency. Such a different behavior can be the consequence of the unsual high-salt concentration (3.6 M NaCl) required to unmask the intrinsic GTPase of *Ss*EF-1α (*2*). In regards to *Ss*EF-2, an opposite effect was observed because the A26G replacement increased its intrinsic GTPase stimulated by ethylene glycol and $BaCl_2$ (*16*). Compared to *Ss*EF-1α wt, the reduced GTPase^{Na} of G13A*Ss*EF-1α can be explained also by the energetic parameters of activation of the reaction, as shown by the increase in the free energy of activation and a less favorable entropic factor found for the GTPase^{Na} of G13A*Ss*EF-1α.

Surprisingly, kirromycin that did not stimulate the GTPase^{Na} of SsEF-1α is able to stimulate the GTPase^{Na} of G13A*Ss*EF-1α (Figure 5). However, the affinity of the mutant toward the antibiotic was 1 order of magnitude lower than that determined for eubacterial EF-Tu (*25*). However, kirromycin was incapable of stimulating the GDP/GTP exchange reaction on both *Ss*EF-1α and G13A*Ss*EF-1α, even though a stimulation by kirromycin of the nucleotide exchange on G13A*Ss*EF-1α cannot be excluded because the GDP/GTP exchange rate on G13A*Ss*EF-1α was very fast, even in the absence of the antibiotic. In addition, under the experimental conditions used in this work, kirromycin was not able to inhibit poly(Phe) synthesis supported by both *Ss*EF-1α and G13A*Ss*EF-1α (not shown). These results agree with the previous observation that protein synthesis in archaea is not inhibited by 100 μM kirromycin at 72 °C (*26*, *27*). Such a different behavior between eubacterial EF-Tu and archaeal EF-1α toward kirromycin was interpreted to be due to different architectures which made archaeal EF-1α different from eubacterial EF-Tu (*23*). Among the eight amino acid residues that, in *E. coli* EF-Tu, were involved in the binding of kirromycin (*28*−*30*), only A375 is conserved in *Ss*EF-1α as A410 (*3*). Therefore, it is possible that, in *Ss*EF-1α, the G13A mutation unmasks other structural features which are recognized by the antibiotic. This possibility is supported by the fact that eukaryal EF-1α from calf brain, phylogenetically closer to archaeal EF-1α rather than to eubacterial EF-Tu, is sensitive to 70 μM kirromycin, although, in such a case, the antibiotic inhibits the intrinsic GTPase of EF-1α (*31*).

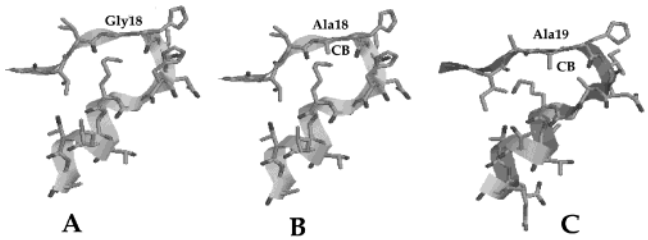

FIGURE 9: Three-dimensional structure of *Ta*EF-Tu·GDP and *Tt*EF-G·GDP in the P-loop region: (A) *Ta*EF-Tu·GDP, (B) *Ta*EF-Tu·GDP after the substitution of Gly18 by Ala, and (C) *Tt*EF-G·GDP (PDB entry 1DAR). Models were visualized by using the RasMol software.

Regarding the effect produced by the G13A replacement on the thermostability of *Ss*EF-1α, only a marginal impairment was observed by monitoring the residual [^{3}H]GDP binding (Figure 7A), UV melting (Figure 7B), or CD denaturation curves (Figure 7C). In addition, these findings indicated that the thermal denaturation process of both *Ss*EF-1α and G13A*Ss*EF-1α involves the entire molecule and not the catalytic domain only. A similar result was also found for *Ss*EF-2, where the A26G replacement did not alter the thermostability of the enzyme (*16*).

To explain on a structural basis the effect of the G13A substitution in *Ss*EF-1α, the 3D strucures in the P-loop region of *Ta*EF-Tu·GDP and *Tt*EF-G·GDP were compared (Figure 9). In *Ec*EF-Tu (Figure 9A), the likely function of the first invariant glycine (Gly18) is to allow an unusual conformation of the main chain (*5*). The modeling of the 3D structure of *Ta*EF-Tu by introducing the G18A substitution reveals an orientation of the methyl group of Ala18 (CB in Figure 9B) toward the α helix containing the consensus elements which interact with GDP, thus resembling what occurs in the 3D structure of *Tt*EF-G (Figure 9C). Although (also in *Tt*EF-G) Ala19 is not involved in the interaction with GDP, it is possible that, in *Ss*EF-1α, the methyl group introduced by the corresponding G13A substitution will cause hydrophobic interactions, making the P-loop region more rigid, thus increasing the affinity of the mutant enzyme toward GDP and GTP but reducing its ability to hydrolyze GTP. This possibility seems supported by the effects observed on the biochemical properties of *Ss*EF-2. The removal of a methyl group by the A26G substitution makes the P-loop region more flexible; therefore, the mutated *Ss*EF-2 showed an increased GTPase activity (*16*).

In conclusion, the reduced ability of G13A*ss*EF-1α to support [^{3}H]Phe polymerization can be ascribed at least to two main reasons: (i) reduced capability to form the ternary complex with eterologous aa-tRNA and (ii) reduced GTPase activity. Finally, the overall results reported in this work indicated that the first amino acid residue in the consensus

sequence G13XXXXGK[T,S] of *Ss*EF-1α or A26XXXXGK-[T,S] of *Ss*EF-2 (*16*) is important for the catalytic properties of the two enzymes. In fact, when glycine is present in this position, both factors display the maximum intrinsic GTPase; vice versa, when alanine is present, the hydrolytic activity is significantly reduced.

REFERENCES

1. Masullo, M., Raimo, G., Parente A., Gambacorta, A., De Rosa, A., and Bocchini, B. (1991) *Eur. J. Biochem. 199*, 529−537.
2. Masullo, M., De Vendittis, E., and Bocchini, V. (1994) *J. Biol. Chem. 269*, 20376−20379.
3. Arcari, P., Gallo, M., Ianniciello, G., Dello Russo, A., and Bocchini, V. (1994) *Biochim. Biophys. Acta 1217*, 333−337.
4. Dever, T. E., Glynias, M. J., and Merrick, W. C. (1987) *Proc. Natl. Acad. Sci. U.S.A. 84*, 1814−1818.
5. Kjeldgaard, M., and Nyborg, J. (1992) *J. Mol. Biol. 223*, 721−742.
6. Berchtold, H., Reshetnikova, L., Reiser, C. O. A., Schirmer, N. K., Sprinzl, M., and Hilgenfield, R. (1993) *Nature 365*, 126−132.
7. Nissen, P., Kjeldgaard, M., Thirup, S., Polekhina, G., Reshetnikova, L., Clark, B. F., and Nyborg, J. (1995) *Science 270*, 1464−1472.
8. Polekhina, G., Thirup, S., Kjeldgaard, M., Nissen, P., Lippmann, C., and Nyborg, J. (1996) *Structure 4*, 1141−1151.
9. Song, H., Parson, M. R., Rowsell, S., Leonard, G., and Phillips, S. E. (1999) *J. Mol. Biol. 285*, 1245−1256.
10. Czworkowski, J., Wang, J., Steitz, T. A., and Moore, P. B. (1994) *EMBO J. 13*, 3661−3668.
11. Ævarsson, A., Brazhnikov, E., Garber, M., Zaeltonosova, J., Chirgadze, Yu., Al-Karadaghi, S., and Liljas, A. (1994) *EMBO J. 13*, 3669−3677.
12. Andersen, G. R., Pedersen, L., Valente, L., Chatterjee, I. I., Kinzy, T. G., Kjeldgaard, M., and Nyborg, J. (2000) *Mol. Cells 5*, 1261−1266.
13. Ævarsson, A. (1995) *J. Mol. Biol. 41*, 1096−1104.
14. Kjeldgaard, M., Nyborg, J., and Clark, B. F. C. (1996) *FASEB J. 10*, 1347−1368.
15. Al-Karadaghi, S., Ævarsson, A., Garber, M., Zaeltonosova, J., and Liljas, A. (1996) *Structure 4*, 555−565.
16. De Vendittis, E., Adinolfi, B. S., Amatruda, M. R., Raimo, G., Masullo, M., and Bocchini, V. (1999) *Eur. J. Biochem. 262*, 600−605.
17. Ianniciello, G., Masullo, M., Gallo, M., Arcari, P., and Bocchini, V. (1996) *Biotechnol. Appl. Biochem. 23*, 41−45.
18. Maniatis, T., Fritsch, E. F., and Sambrook, J. (1982) *Molecular Cloning. A Laboratory Manual*, Cold Spring Harbor Laboratory, Plainview, NY.
19. Studier, F. W., Rosemberg, A. H., Dunn, J. J., and Dubendorff, J. W. (1990) *Methods Enzymol. 185*, 60−89.
20. Masullo, M., Ianniciello, G., Arcari, P., and Bocchini, V. (1997) *Eur. J. Biochem. 243*, 468−473.
21. Arcari, P., Masullo, M., Arcucci, A., Ianniciello, G., de Paola, B., and Bocchini, V. (1999) *Biochemistry 38*, 12288−12295.
22. Raimo, G., Masullo, M., Lombardo, B., and Bocchini, V. (2000) *Eur. J. Biochem. 267*, 6012−6017.
23. Raimo, G., Masullo, M., Savino, G., Scarano, G., Ianniciello, G., Parente, A., and Bocchini, V. (1996) *Biochim. Biophys. Acta 1293*, 106−112.
24. Guex, N., and Peitsch, M. C. (1997) *Electrophoresis 18*, 2714−2723.
25. Masullo, M., Arcari, P., de Paola, B., Parmeggiani, A., and Bocchini, V. (2000) *Biochemistry 39*, 15531−15539.
26. Cammarano, P., Teichner, A., Chinali, G., Londei, P., de Rosa, M., Gambacorta, A., and Nicolaus, B. (1982) *FEBS Lett. 148*, 255−259.
27. Cammarano, P., Teichner, A., Londei, P., Acca, M., Nicolaus, B., Sanz, J. L., and Amilis, R. (1985) *EMBO J. 4*, 811−816.
28. Abdulkarim, F., Liljas, L., and Hughes, D. (1994) *FEBS Lett. 352*, 118−122.
29. Mesters, J. R., Zeef, L. A. H., Hilgenfeld, R., de Graaf, J. M., Kraal, B., and Bosch, L. (1994) *EMBO J. 13*, 4877−4855.
30. Vogeley, L., Palm, G. J., Mesters, J. R., and Hilgenfeld, R. (2001) *J. Biol. Chem. 276*, 17149−17155.
31. Crechet, J. B., and Parmeggiani, A. (1986) *Eur. J. Biochem. 161*, 655−660.

BI015598H